Response to Referee #2

The manuscript addresses a scientifically important and potentially novel upstream–downstream linkage between South Asian aerosol transport, ice-phase cloud development over Mount Qomolangma, and precipitation over downstream East Asia. The study extends from local aerosol–cloud–precipitation interactions to the upstream–downstream linkages between the Plateau and eastern China, with significant scientific questions and high potential impact. However, the conceptual strength of the conclusion is far higher than the strength of the evidence. The central claim of a long-range ice-crystal seeding effect is presently inferred from spatial and temporal covariability rather than directly demonstrated. Major confounding by large-scale circulation and moisture transport has not been adequately controlled, the physical continuity and survival of transported ice crystals have not been established, and several aspects of the event selection and statistical analysis require fundamental revision.

"Despite these impacts, the intricate interactions between aerosol and cloud microphysics make the effects of aerosol on precipitation poorly understood (Levin and Cotton 2009; IPCC Climate Change 2013)。"The author summarizes the gaps in existing research in the Introduction, but this is only a broad background issue. In fact, the specific problem analysis of this study is not deep enough; this statement only addresses the general issue that the impact of current aerosols on rainfall is unclear, but does not focus on what specific problem this study intends to investigate in depth. In addition, the cited research analysis is insufficient, the literature is relatively outdated, and the IPCC has already released new reports.

Response 1： Following the suggestion of reviewer, we have cited the recent literature in the revised manuscript as follows:

Lines 93-108: Aerosols acting as CCN and INPs may alter cloud droplet activation, promote heterogeneous ice nucleation, and modify the partitioning among liquid, supercooled-liquid, mixed-phase, and ice-phase clouds (Zhu et al., 2024). A small subset of atmospheric aerosol particles can act as INPs and initiate heterogeneous ice formation in ice-phase clouds through immersion, deposition, contact, or condensation freezing. Mineral dust and soot particles are regarded as the primary atmospheric INP types. Once primary ice crystals are generated, depositional growth, riming, the Wegener-Bergeron-Findeisen process (Wegener, 1911; Bergeron, 1935; Findeisen, 1938), and secondary ice production can further amplify cloud glaciation and modify the partitioning between liquid and ice water (Murray et al., 2012). Nevertheless, aerosol concentration alone does not directly represent INP abundance, and the observed aerosol–ice-cloud relationship may also be affected by temperature, humidity, vertical motion, and cloud dynamics (Zhu et al., 2024; Xu et al. 2025). Atmospheric aerosols interact with clouds through tightly coupled microphysical, radiative, thermodynamic, and dynamical processes. Vertical motion, moisture availability, temperature and large-scale circulation are meteorological factors that collectively determine whether elevated aerosol loading stimulates or inhibits cloud and precipitation development. Therefore, the ice-phase clouds could be interpreted as the combined result of aerosol-mediated ice nucleation and favorable thermodynamic and dynamical conditions, rather than as an aerosol effect alone. These interactions are highly nonlinear and depend strongly on cloud type, cloud evolutionary stage, and the surrounding meteorological environment（IPCC, 2023）.

References

Bergeron, T.: On the physics of cloud and precipitation, in: Proceedings of the Fifth Assembly of the International Union of Geodesy and Geophysics, Lisbon, Portugal, IUGG, 156–178, 1935.

Findeisen, W.: Die Kolloidmeterorologischem Vorgange der Niedershlagsbildung, Meteorol. Z., 55, 121–133, 1938.

Intergovernmental Panel on Climate Change. Climate Change 2021 – The Physical Science Basis: Working Group I Contribution to the Sixth Assessment Report of the Intergovernmental Panel on Climate Change (1st ed.), Cambridge University Press (2023), https://doi.org/10.1017/9781009157896

Murray, B. J., O'Sullivan, D., Atkinson, J. D., and Webb, M. E.: Ice nucleation by particles immersed in supercooled cloud droplets, Chem. Soc. Rev., 41, 6519–6554, https://doi.org/10.1039/c2cs35200a, 2012.

Wegener, A.: Thermodynamik der Atmosphäre, J. A. Barth, Leipzig, 331 pp., https://doi.org/10.1038/090031a0, 1911.

Zhu, S. Z., Qian, L., Ma, X. Q., Qiu, Y. J., Yang, J., He, X., Li, J. J., Zhu, L., Gong, J., and Lu, C. S.: Impact of Aerosols on the Macrophysical and Microphysical Characteristics of Ice-Phase and Mixed-Phase Clouds over the Tibetan Plateau, Remote Sens., 16, 1781, https://doi.org/10.3390/rs16101781, 2024.

2. The authors synthesized and compared high-AEC days and low-AEC days, and attributed the differences in ice-phase clouds, latent heat, and precipitation to aerosol effects. However, South Asian monsoon moisture transport, vertical motion, humidity, and cloud cover determine both the AEC in the Everest region and the formation of ice-phase clouds and downstream precipitation. In observational studies, separating aerosol effects from meteorological covariation is one of the difficulties in aerosol–cloud research, but simple grouping, correlation, or spatial overlap usually cannot provide causal attribution.

Response 2： From thermodynamic and dynamic perspectives, Xu et al. (2025) elucidated the relationships between AEC levels over the MQ and the associated atmospheric dynamic and thermodynamic conditions, as well as the complex relationships between heavy precipitation over the MQ region and vertical motion, water vapor, humidity, aerosols, and other relevant factors. They found pronounced differences in the vertical dynamic and thermodynamic structures associated with high- and low-aerosol-loading transport episodes over the MQ (Figs. 2c and 2d), which were accompanied by substantial differences in cloud-phase composition.

As shown in Table 1, during high-aerosol-loading episodes, strong ascending motion driven by intense diabatic heating enabled clouds to develop to greater altitudes, allowing large numbers of cloud droplets to be lifted above the freezing level and converted into ice-phase clouds. Consequently, the occurrence frequencies of supercooled-liquid, mixed-phase, and ice-phase clouds were significantly higher during high-aerosol-loading episodes than during low-aerosol-loading episodes. By contrast, liquid-phase clouds occurred more frequently during low-aerosol-loading episodes. On the basis of the differences in atmospheric vertical dynamic structures arising from the Q_1 feedback effects associated with high- and low-aerosol-loading transport episodes, Xu et al. (2025) further examined the relationships among precipitation on the southern and northern slopes of MQ, AEC measured at the MQ lidar station, and the intensity of dynamical lifting, represented by vertical velocity and Q_1, during July 2018 and July 2019 (Fig. 3). Although most precipitation events on both slopes occurred under conditions characterized by strong dynamical lifting, large Q_1 values, and high AEC, the influence of aerosols on precipitation was more pronounced on the northern slope than on the southern slope under comparable lifting conditions.

As shown in Table 2, under similar dynamical lifting conditions ($\omega > 0.0 \times 10^{-2}$ Pa s^{-1} d^{-1}), precipitation events exceeding 25 mm d^{-1} occurred on the northern slope when the AEC anomaly was greater than or equal to 0.0 km^{-1} d^{-1}. Comparisons of AEC with relative humidity and precipitation on the southern and northern slopes further revealed significant logarithmic relationships between AEC and relative humidity on both slopes. Interestingly, most relatively intense precipitation events exceeding 10 mm d^{-1} on the northern slope occurred during periods when AEC increased rapidly while the increase in relative humidity gradually leveled off (Figs. 4a and 4b). In contrast, at Nyalam Station on the southern slope, where persistently humid conditions prevailed, high AEC values were mostly associated with weak precipitation (Fig. 4c).

The mean hourly precipitation intensity for different AEC categories showed a clear increasing trend with increasing AEC at the two northern-slope stations, whereas hourly precipitation intensity on the southern slope fluctuated only slightly as AEC increased (Fig. 4d). Clouds influenced by aerosol activation also exhibited more vigorous development. A comparison of the responses of convective-cloud development to lower-tropospheric aerosols and water vapor indicated that convective-cloud development over the MQ region was not primarily controlled by atmospheric moisture conditions. Its response to water vapor was considerably weaker than its response to AEC (Fig. 5). These results further support the conclusion that aerosol activation can make aerosols a key factor governing the evolution of convective clouds.

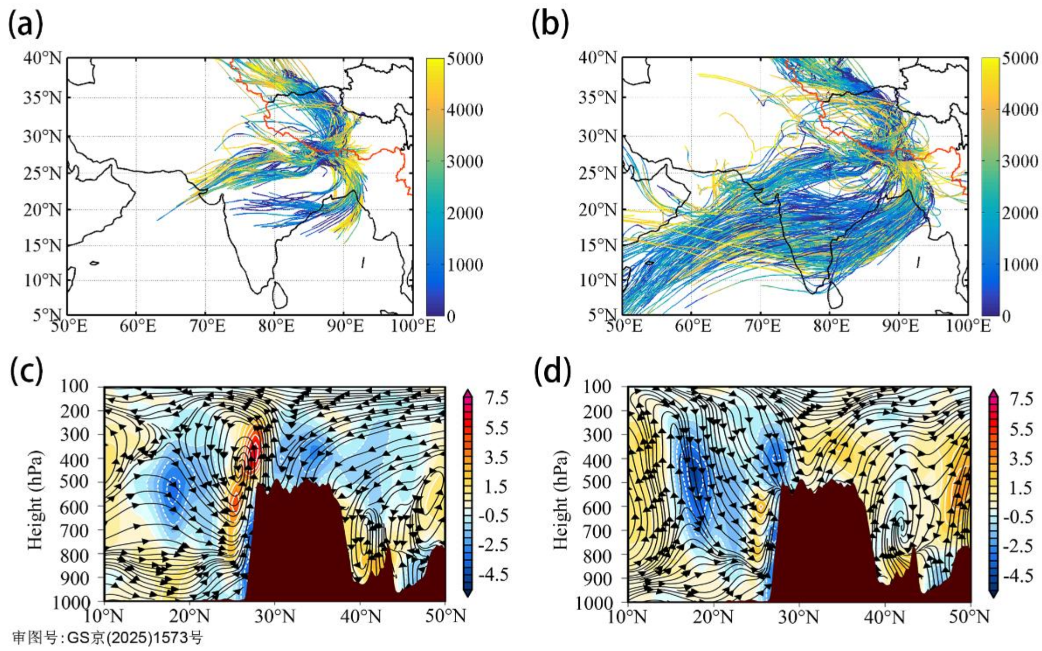

Fig. 2. The thermal-dynamic mechanism of aerosol activation effect on the cloud-precipitation process and aerosol transport (Xu et al., 2025). (a) 3-day and (b) 6-day backward trajectories of the high-concentration aerosol transport to the MQ in the vertical altitudes over ground (in unit of m with color lines) in July 2018 and July 2019; The meridional-vertical sections of anomalous vertical circulations (stream lines of v- and - $\omega\times10^2$ components) and anomalous atmospheric apparent heat sources Q_1 averaged (10^{-5} w/kg, color contours) over 86°-90°E at (c) high-concentration and (d) low-concentration aerosol process over the MQ in July 2018 and July 2019.

Table 1 The occurrence rates (%) of cloud phases with liquid droplets, supercooled liquid droplets, ice particles and the liquid-ice mix during the high-and low-level aerosol processes over the MQ region in July 2018 and July 2019 (Xu et al., 2025).

	LD	**SLD**	**IP**	**LIM**
HL	**5.1**	**21.8**	**55.8**	**17.3**
LL	**21.3**	**21.2**	**47.6**	**9.9**

* liquid droplets (LD), supercooled liquid droplets (SLD), ice particles (IP) and the liquid-ice mixing (LIM) during the high-level (HL) and low-level (LL) aerosol processes

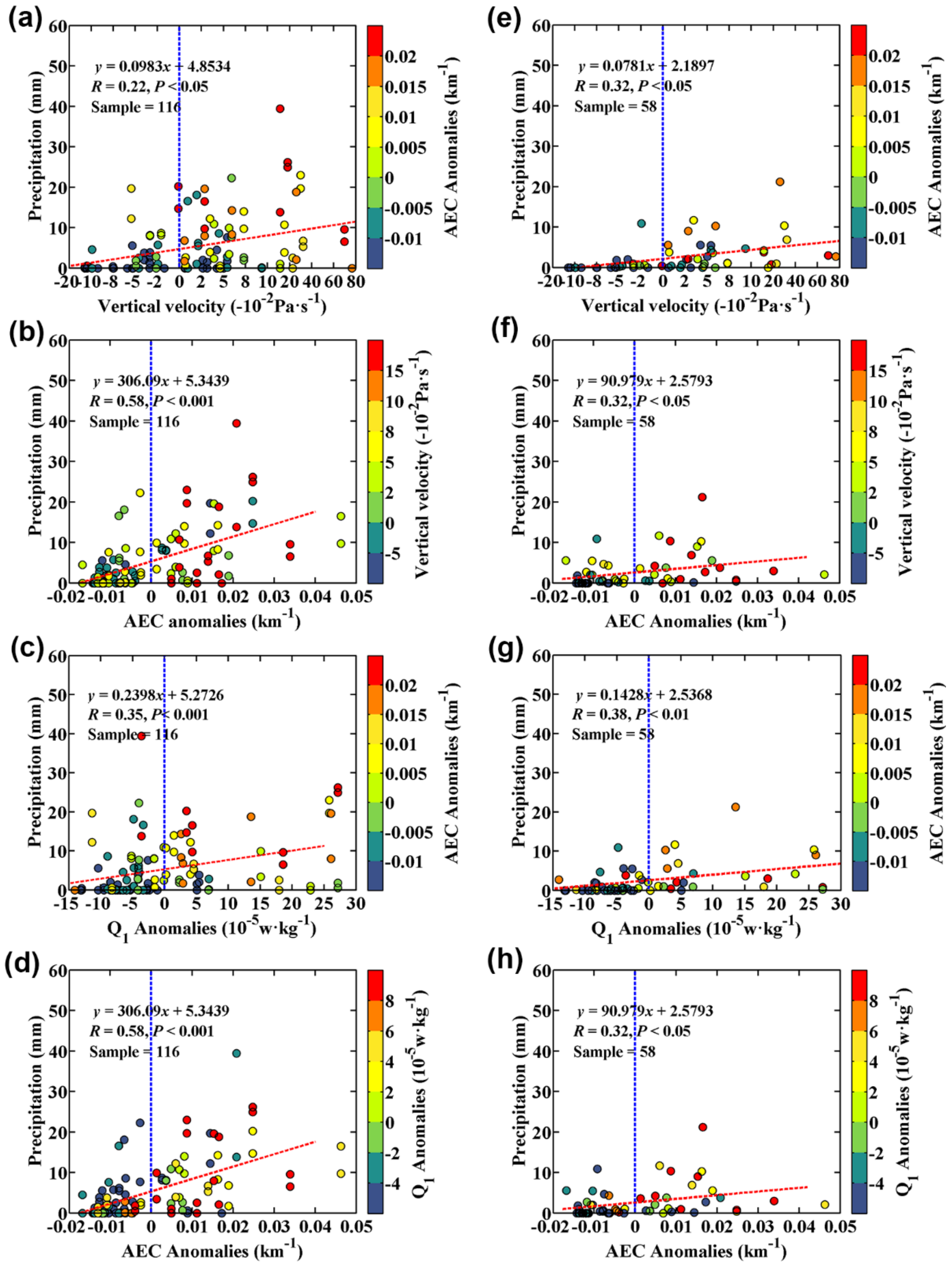

Fig. 3. Relationships among precipitation and aerosols, atmospheric dynamic uplift intensity (Xu et al., 2025). Scatter plots of precipitation over the south and north slopes of the MQ with (a, e) the vertical velocity (ω), and (c, g) Q_1 anomalies as well as (b, d, f, h) the AEC anomalies in July 2018 and July 2019 with (a-d) the north slope precipitation, (e-h) the south slope precipitation, (a, c, e, g) AEC anomalies (color shade), (b, f) vertical velocity (color shades), (d, h) Q_1 anomalies (color shade). Red dash lines are the linear fitting lines, and blue dash lines are zero-value lines. The AEC anomalies refer to the deviations of daily averages of AEC values from the average AEC for July 2018 and July 2019. The Q_1 anomalies refer to the deviations of daily averages of AEC values from the average Q_1 for July 2018 and July 2019 with the vertical velocity in daily mean values, and the precipitation in daily accumulated values.

Table 2 Difference of rainy day probability between the south slope and the north slope of the MQ under the same atmospheric uplift conditions with the daily averages of $\omega > 0.0$ (ω in unit of $-10^{-2} Pa \cdot s^{-1}$) in the different aerosol concentrations (Xu et al., 2025).

Daily **precipitation levels (mm)**	**Probability of rainy day**			
	AEC anomalies ≥ 0.0 km^{-1}		**AEC anomalies < 0.0 km^{-1}**	
	North slope	**South slope**	**North slope**	**South slope**
[0.1, 10)	**60.0%**	**78.9%**	**85.0%**	**100.0%**
[10.0, 25.0)	**34.3%**	**21.1%**	**15.0%**	——
≥25.0	**5.7%**	——	——	——

* The AEC anomalies refer to the deviations of daily averages of AEC values from the average AEC for July 2018 and July 2019. Positive anomalies indicate relatively heavy pollution, while negative anomalies correspond to lighter pollution levels. There are 116 samples at the north slope and 58 samples at the south slope of the MQ in July 2018 and July 2019.

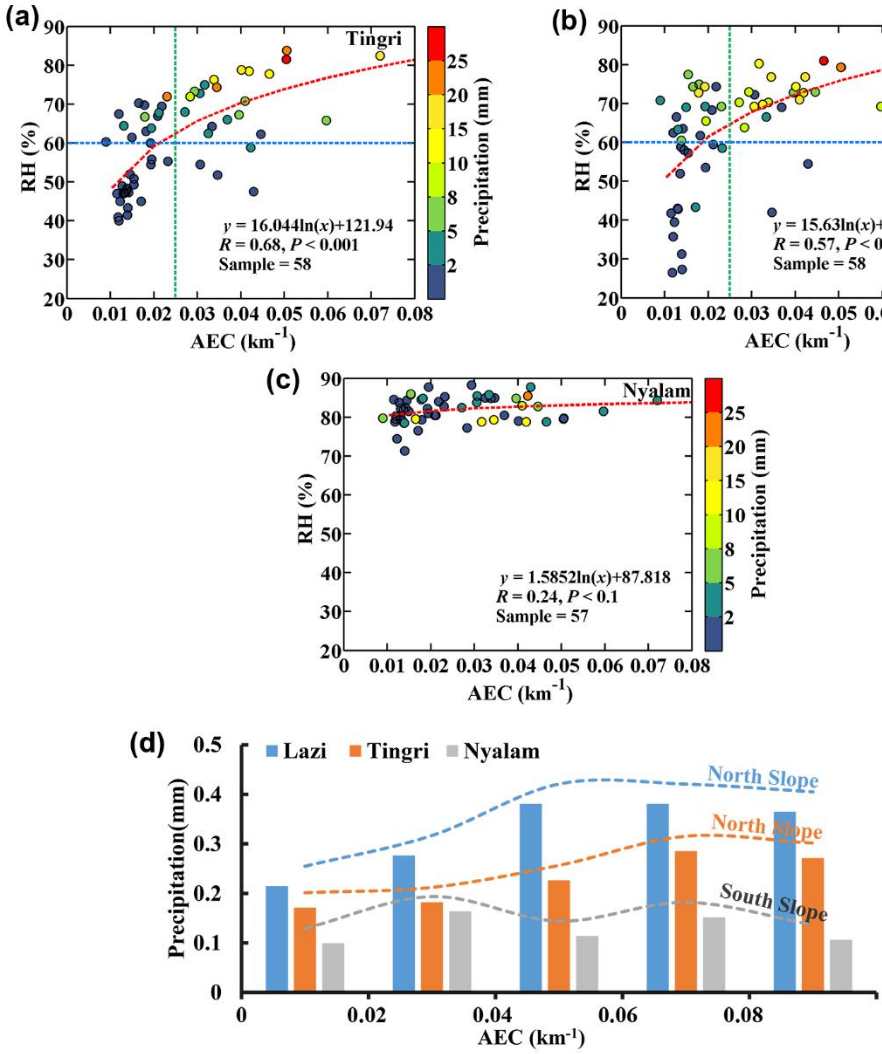

Fig. 4. Relationships among aerosols, RH and precipitation (Xu et al., 2025). Correlations of RH and the AEC in July 2018 and July 2019 at (a) Tingri Station, (b) Lazi Station and (c) Nyalam Station with color shade for daily precipitation, the fitting lines (red dash lines), the green dash lines for AEC = 0.025 km^{-1}, and the blue dash lines for RH = 60% with RH and AEC in daily mean values, and the precipitation in daily accumulated values. (d) Hourly precipitation intensity in different AEC (hourly means) ranges at Tingri (orange color), Lazi (blue color) and Nyalam (grey color) Stations with the dashed lines presenting the hourly precipitation intensity with AEC change.

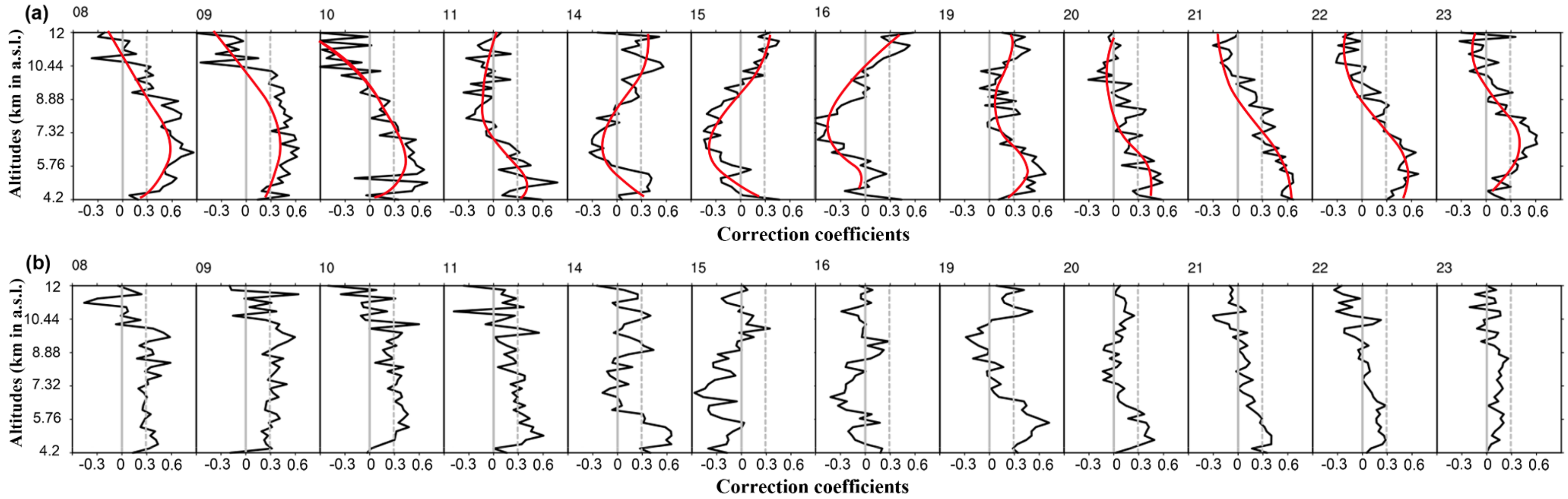

Fig. 5. Hourly changes from 08 in the responses of deep convective clouds on the MQ to (a) lower-atmospheric AEC and (b) vapor at 500 hPa (Xu et al., 2025). The x-arises present the lag correction coefficients of vertical structures of X-band dual-polarization weather radar echo reflectivity with the AEC averaged during 00:00 to 07:00 over the altitudes of 0.15-2.5 km in the upper panel and the specific humidity at 500 hPa averaged during 00 to 07 in the lower panel, and the y-arises denote the altitudes (km in a.s.l.) with zero correction (solid straight lines) and the significance level of 0.1 (dash straight lines). The solid red lines represent the change patterns of the relevant profiles. Only X-band dual-polarization weather radar and Lidar observational data from July 2019 were employed. The hourly changes in the responses of deep convective clouds on the MQ to lower-atmospheric AEC and vapor at 500 hPa are detailed in Fig. S4 (online).

Building upon the work of Xu et al. (2025), the present study focuses on the activation effect of externally transported aerosols on ice-phase clouds. By comparing the differences in cloud phase, latent heat release, and cloud–precipitation processes between high- and low-aerosol-loading episodes during July 2018 and July 2019, we specifically investigate how externally transported aerosols over the MQ region can promote the formation of ice-phase clouds under different large-scale atmospheric circulation patterns. We further demonstrate that these aerosol-influenced ice clouds can be efficiently transported downstream along preferred pathways, thereby exerting a pronounced ice-crystal seeding effect on downstream cloud-to-precipitation conversion.

Cloud-phase retrievals from the FY-4A satellite further indicate that the occurrence frequencies of ice-phase clouds, supercooled liquid clouds, and mixed-phase clouds are all higher under high-aerosol-loading conditions than under low-aerosol-loading conditions. In contrast, liquid-phase clouds occur much more frequently during low-aerosol-loading episodes than during high-aerosol-loading episodes (Fig. 1c). Compared with liquid clouds, ice clouds occur more frequently over the Tibetan Plateau and exhibit a stronger association with aerosol loading, consistent with previous observational and modeling studies (Hua et al., 2020).

A comprehensive analysis of the diurnal variations in aerosol extinction coefficient derived from lidar observations, the maximum reflectivity observed by the X-band dual-polarization radar, and the occurrence frequencies of different cloud phases revealed that aerosol loading was significantly and positively correlated only with the occurrence frequencies of ice-phase and mixed-phase clouds, whereas no statistically significant relationship was found with liquid-phase or supercooled liquid clouds (Figs. 1d and 1e). Furthermore, the diurnal variations of ice-phase and mixed-phase cloud frequencies exhibited coherent peaks and troughs with the diurnal evolution of maximum radar reflectivity (Figs. 1d and 1e), suggesting that these cloud types are closely associated with aerosol-enhanced deep convective development.

These results indicate that increased aerosol loading is associated with enhanced occurrences of ice-phase and mixed-phase clouds within deep convective systems, whereas lower aerosol-loading conditions are generally accompanied by a higher persistence of liquid-phase clouds. To further clarify the relationships between aerosol effects and meteorological factors, we have incorporated the findings of our previous study into the Introduction, as follows:

Line 61-62： Over the Tibetan Plateau (TP), aerosol–cloud–precipitation interactions are particularly important because externally transported aerosols can be lifted rapidly by strong topographic and convective ascent (Xu et al. 2025).

Line 68-92： The Mount Qomolangma (MQ) as a natural laboratory for investigating aerosol–cloud–precipitation interactions over the TP (Xu et al. 2025). During the MQ aerosol–cloud–precipitation integrated vertical observation campaign, Xu et al. (2025) showed that, during the Indian summer monsoon, aerosols transported from South Asia exerted a pronounced activation effect on cloud and precipitation processes. Under dynamically forced lifting conditions, enhanced aerosol loading suppressed and delayed weak precipitation over MQ while promoting more vigorous cloud development, ultimately resulting in increased precipitation on the northern slope. The synergistic interaction between the thermodynamic–dynamic forcing over MQ and aerosol activation favored the development of deep convection associated with precipitation on the northern slope. Aerosol activation also enhanced cloud development. Convective-cloud development over the MQ region was found to be more responsive to aerosol than to atmospheric moisture conditions, suggesting that aerosol activation plays a key role in regulating the evolution of convective clouds (Xu et al. 2025).

From thermodynamic and dynamic perspectives, Xu et al. (2025) further elucidated the relationships between AEC levels over MQ and the associated atmospheric dynamic and thermodynamic conditions, as well as the complex relationships between heavy precipitation and meteorological factors, including vertical motion, water vapor, humidity, and aerosols. High-aerosol-loading episodes were characterized by a stronger apparent heat source (Q_1) than low-aerosol-loading episodes, thereby enhancing ascending motion over the southern slope of MQ. Over the TP and its surrounding regions, transported soot and dust aerosols have been linked to variations in ice-crystal effective radius, ice water content, cloud optical properties, and cloud-phase partitioning (Liu et al. 2019). Under these distinct dynamic and thermodynamic conditions, the occurrence frequencies of ice-phase and mixed-phase clouds were significantly higher during high-aerosol-loading episodes than during low-aerosol-loading episodes (Xu et al. 2025).

Line 116-118: Therefore, under favorable thermodynamic and dynamic conditions, aerosol-influenced cloud particles and ice crystals may be transported downstream, potentially affecting cloud-to-precipitation conversion beyond the aerosol source region.

References

Liu, Y. Z., Hua, S., Jia, R., and Huang, J. P.: Effect of aerosols on the ice cloud properties over the Tibetan Plateau, J. Geophys. Res.: Atmos., 124, 9594–9608, https://doi.org/10.1029/2019JD030463, 2019.

Xu, X. D., Cai, W. Y., Zhao, T. L., Zhang, H., Guo, X. L., Liu, W. Q., Zhang, T. S., Zhao, R. Z., Wu, C., Li, Y. Q., Wang, L., Yan, P., and Yang, C. J.: Understanding clouds and precipitation over the Mount Qomolangma: how does the aerosol activation effect exist?, Sci. Bull., 70, 3649–3658, https://doi.org/10.1016/j.scib.2025.09.031, 2025.

3. *The authors attribute cloud phase anomalies at scales of hundreds to thousands of kilometers and lasting 1–3 days to the direct transport of ice crystals from Mount Everest, but provides no calculations of ice crystal trajectories, transport speeds, settling velocities, sublimation losses, or continuity of ice water content.*

The authors use single-site AEC and MODIS AOD to infer that aerosols originate from South Asia, and further claims that high concentrations of carbonaceous aerosols act as efficient ice nuclei to promote ice formation. I think it is necessary to include trajectory clustering, potential source contribution analysis, or satellite/reanalysis aerosol type data.

Response 3： The aerosol transport path and potential source areas from South Asia and the surrounding regions to the MQ are confirmed by the synthesized backward trajectories of high-concentration aerosol processes in July 2018 and July 2019 (Xu et al. (2025)). Here, the inference based on the relationship between the single-site AEC and MODIS AOD was intended not only to demonstrate that aerosols over the MQ originated from South Asia, but also to show that aerosol variations over the MQ were consistent with those over South Asia.

Following the reviewer's suggestion, we have added the accumulated distributions of ice-phase clouds during the preceding 48 h for each day from 9 to 11 July 2018, together with FLEXPART forward-trajectory simulations for this high-aerosol-loading episode (Fig. S2). Comparative analysis shows that the evolution of precipitation during 9–11 July 2018 (Figs. S2b–d) is consistent with both the evolving distributions of ice-phase clouds (Figs. S2e–g) and the FLEXPART-simulated forward trajectories (Fig. S2h). As the episode progressed, most FLEXPART trajectories were transported at upper levels. These trajectories were also similar to the latent-heat transport pathways indicative of ice clouds or ice crystals (Figs. 2a and 2b), as well as to the spatial distributions of ice-phase and mixed-phase cloud anomalies under high- and low-aerosol-loading conditions in July 2018 and July 2019 (Fig. S1).

The following text has therefore been added to Lines 326-329 of the revised manuscript:

"Comparative analysis shows that the evolution of precipitation during 9–11 July 2018 (Figs. S2b–d) is consistent with both the evolving distributions of ice-phase clouds (Figs. S2e–g) and the FLEXPART-simulated forward trajectories (Fig. S2h). As the episode progressed, most FLEXPART trajectories were transported at upper levels.”

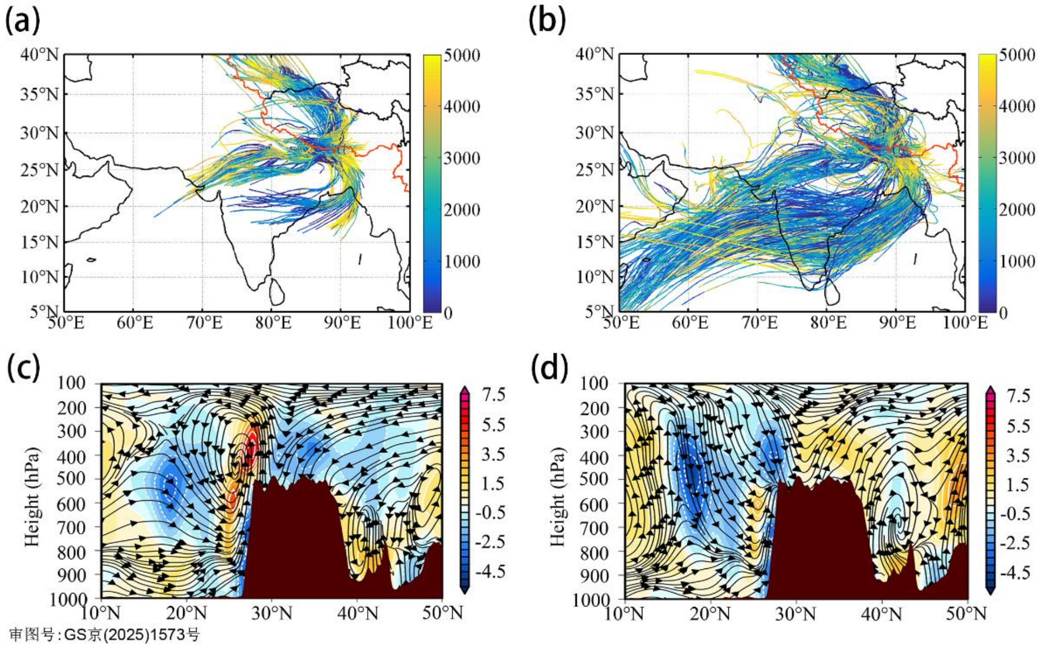

Fig. 2. The thermal-dynamic mechanism of aerosol activation effect on the cloud-precipitation process and aerosol transport (Xu et al., 2025). (a) 3-day and (b) 6-day backward trajectories of the high-concentration aerosol transport to the MQ in the vertical altitudes over ground (in unit of m with color lines) in July 2018 and July 2019; The meridional-vertical sections of anomalous vertical circulations (stream lines of v- and - $\omega\times10^2$ components) and anomalous atmospheric apparent heat sources Q_1 averaged (10^{-5} w/kg, color contours) over 86°-90°E at (c) high-concentration and (d) low-concentration aerosol process over the MQ in July 2018 and July 2019.

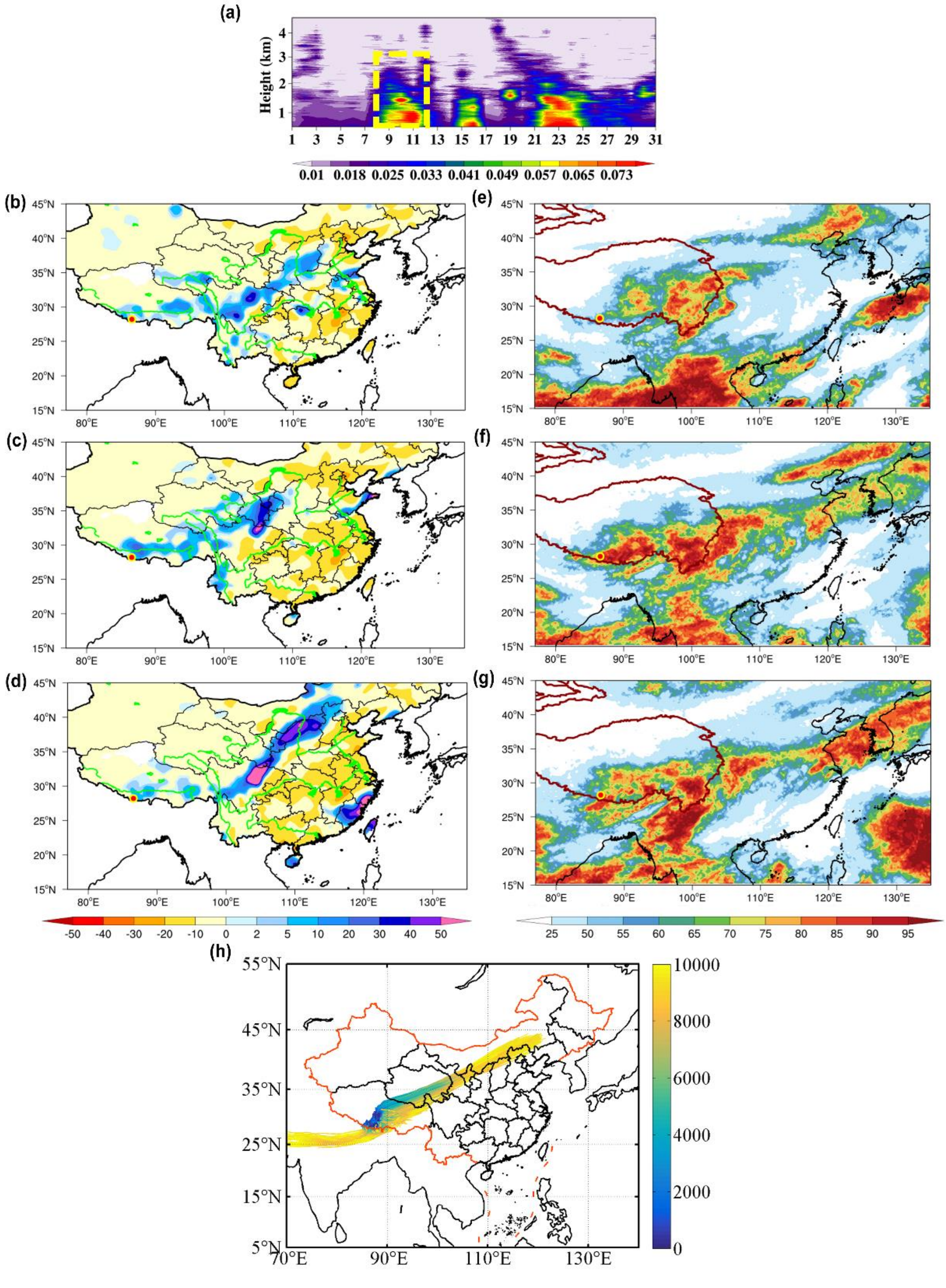

Figure S2. (a) Daily variations in the aerosol extinction coefficient over Mount Qomolangma in 2018. The yellow box indicates the selected high-aerosol-loading episode from 9 to 11 July 2018. (b–d) Evolution of precipitation in the upstream and downstream regions on the day of the high-aerosol-loading event and during the following two days. (e–g) Spatial distributions of ice-phase clouds accumulated over the preceding 48 h for each day of the event. Panels (b, e), (c, f), and (d, g) correspond to the event day, the following day, and the second day after the event, respectively. (h) FLEXPART-simulated forward trajectories for the selected episode (in unit of m with color lines).

References

Xu, X. D., Cai, W. Y., Zhao, T. L., Zhang, H., Guo, X. L., Liu, W. Q., Zhang, T. S., Zhao, R. Z., Wu, C., Li, Y. Q., Wang, L., Yan, P., and Yang, C. J.: Understanding clouds and precipitation over the Mount Qomolangma: how does the aerosol activation effect exist?, Sci. Bull., 70, 3649–3658, https://doi.org/10.1016/j.scib.2025.09.031, 2025.

4. The caption of Figure 1 states "90% confidence level (P > 0.1)," and Figure 4 states "95% confidence level (P > 0.05)." The statistical significance should be P < 0.1 and P < 0.05, respectively. This concerns whether the actual calculation of the significance regions used the wrong criteria.

Response 4： Thanks for the careful review. We have accordingly corrected the captions of Figures 1 and 4.